SCIENCE CHINA
Technological Sciences

•Article•

May 2022 Vol.65 No.5: 1149–1159
https://doi.org/10.1007/s11431-020-1817-3

Wear behavior of the raw and pre-smashed carbon nanotubes reinforced 6061Al composites fabricated by powder metallurgy

LI XiaoNan[1,2], LIU ZhenYu[1*], ZAN YuNing, XIAO BoLü[1*], NI DingRui[1], WANG QuanZhao[1], WANG Dong[1] & MA ZongYi[1]

[1] *Shi-changxu Innovation Center for Advanced Materials, Institute of Metal Research, Chinese Academy of Sciences, Shenyang 110016, China;*
[2] *School of Materials Science and Engineering, University of Science and Technology of China, Shenyang 110016, China*

Received December 25, 2020; accepted March 22, 2021; published online March 30, 2022

The raw and pre-smashed (PS) carbon nanotube (CNT) reinforced 6061Al composites (CNT/6061Al) with different CNT contents were respectively fabricated by powder metallurgy technology. It was found that reducing the CNT cluster size by pre-smashing processing could sharply reduce the friction coefficient, and significantly improve the density, hardness, and wear resistance of the CNT/6061Al composites. For the raw-CNT/6061Al composites, the wear rate increased approximately linear trend while the CNT content was over 1 wt.%. The plastic deformation, deep grooves, and serious delamination were presented on the wear surface. The wear process was gradually transformed from Al-copper base counterpart wear into Al-Al wear for the higher adhesion-binding energy between aluminum and copper base counterpart. While for the PS-CNT/6061Al composites, the wear rate gradually decreased as the CNT content increased from 0 to 2 wt.%. This was mainly because the generation of the thinner mechanically mixed layer (MML) and the PS-CNT prevented the direct contact between specimen and copper base counterpart, which effectively inhibited the adhesive wear. But excessive PS-CNT addition (~3 wt.%) would weaken the bonding between CNT and 6061Al, and thus the wear resistance of the composite was reduced apparently.

wear, carbon nanotube, aluminum matrix composites, clustering

Citation: Li X N, Liu Z Y, Zan Y N, et al. Wear behavior of the raw and pre-smashed carbon nanotubes reinforced 6061Al composites fabricated by powder metallurgy. Sci China Tech Sci, 2022, 65: 1149–1159, https://doi.org/10.1007/s11431-020-1817-3

1 Introduction

Aluminum and its alloys have been widely used in the transportation, electric power, and aerospace industry [1–5], for their excellent mechanical properties, high thermal conductivity combined with good electrical conductivity [6–9]. However, aluminum base materials showed poor wear resistance under the boundary lubrication conditions due to the severe adhesion effect without good lubrication. This was the main obstacle to the high performance tribological applications for aluminum base materials, especially in the electric contact field [10]. Recently, the carbon nanotube (CNT) with superior mechanical and physical properties [11–13] has attracted much attention, and many studies indicate that CNT incorporation into Al matrix has a remarkable effect on improving the wear resistance for its unique topological structure [14–23]. Moreover, CNT has been expected to be used in industrial applications for its significantly decreased price [24,25].

Some previous investigators have examined the wear resistance of CNT reinforced aluminum matrix composites (CNT/Al) [15–17,19–21,26]. For example, some studies [16,17,19,26,27] have reported the preparation method and wear behavior, but the CNT dispersion in the composites was not mentioned. The actual dispersion state of CNTs could only be speculated according to the reported preparation

*Corresponding authors (email: zyliu@imr.ac.cn; blxiao@imr.ac.cn)

methods and experimental results. This complicated the relationship between CNT distribution and wear behaviors. Only a few investigators provided the CNT distribution information and simultaneously analyzed the wear behavior of CNT/Al composites. For example, Choi et al. [21] and Bastwros et al. [16] fabricated the well-dispersed CNT/Al composites and found that the well-dispersed CNT/Al composites generally had an excellent wear resistance due to the self-lubrication effect of CNT [20,21]. But for the clustering CNT/Al composites, the reported wear behaviors were of significant difference [15–17,19,26,28]. Yildirim et al. [27] investigated the wear behavior of CNT/7075Al composites with clustering CNT and found that the wear rates of 0.5, 1 wt.% CNT/7075Al composites decreased slightly, while the wear rates significantly increased for the 2, 3, 4 wt.% CNT/7075Al composites. This suggested that only the CNT with low content could slightly increase the wear resistance of composites, but high CNT content was not beneficial in improving wear resistance. However, other researchers reported the opposite results. For example, Kim et al. [17] treated the clustered CNTs by acid treatment as well as ultrasonication mixing and achieved a certain improvement of CNT clustering. Their study showed that adding clustered 5 wt.% CNT could still improve the wear resistance of composite compared with the matrix alloy under a relatively lower applied load. The above indicates that the wear behavior of CNT/Al composites was complicated and still needed to investigate.

On the other hand, CNTs were difficult to be uniformly dispersed into Al matrix alloy [6,7]. The uniformly dispersed CNTs in Al matrix alloy were over dependent on ball milling technology [25,29–31], which had the problem of impurity incorporation and high cost [32]. This was harmful to electrical conductivity and the application of CNT/Al composites in the electric contact field. From this point of view, the CNT/Al composites with the uniformly dispersed CNTs might not be a better choice. Considering the above mentioned, it was still necessary to research the wear behavior of the clustering CNT/Al composites with different dispersion states under different applied loads.

In this study, CNT/6061Al composites with two different dispersion conditions were prepared through powder metallurgy technology. The dispersion conditions of CNT/6061Al composites were controlled by changing the size of CNT clusters through ball milling processing. The CNT distribution, hardness, and wear behavior of CNT/6061Al composites were examined. The aim of the present work was to study the wear behavior of the CNT/6061Al composites with two different dispersion conditions under different applied loads.

2 Experimental

2.1 Raw materials and composite fabrication

The as-received CNT was synthesized using chemical vapor deposition, and it has a purity of about 98%. As the result of the large aspect ratio and strong van der Waals force, the raw CNTs were entangled together into very large clusters (Figure 1(a)), some even reached millimeter level. The magnified image indicates that the CNT had an outer diameter of 10–20 nm and a length of several micrometers (Figure 1(b)). The preparation process flow for fabricating CNT/6061Al composites is shown in Figure 2. The entangled CNT was firstly pre-smashed by ball milling technology using an attritor for 2 h at a rotational speed of 200 r min^{-1}. The hardened steel balls of 5 mm in diameter were used, and the ball to powder ratio was 200:1. Through this way, the pre-smashed CNT (PS-CNT) with smaller cluster sizes was prepared successfully (Figure 1(c)), mainly attributed to the severe shear effect during milling.

The various CNT contents of PS-CNT or raw-CNT (1, 2, and 3 wt.%) were respectively mixed with 6061Al (Al-1.2 wt.% Mg-0.6 wt.% Si-0.2 wt.% Cu) powders in a bi-axis rotary mixer for 6 h at a rotation speed of 60 r min^{-1} with 1:1 ball to powder ratio. Then, the as-mixed PS-CNT/6061Al or raw-CNT/6061Al powders were cold-compacted in a cylinder die, hot pressed at 873 K for 1.5 h into a billet, and finally hot extruded at 723 K with an extrusion ratio of 16:1.

The CNT/6061Al composites were finally solution treated

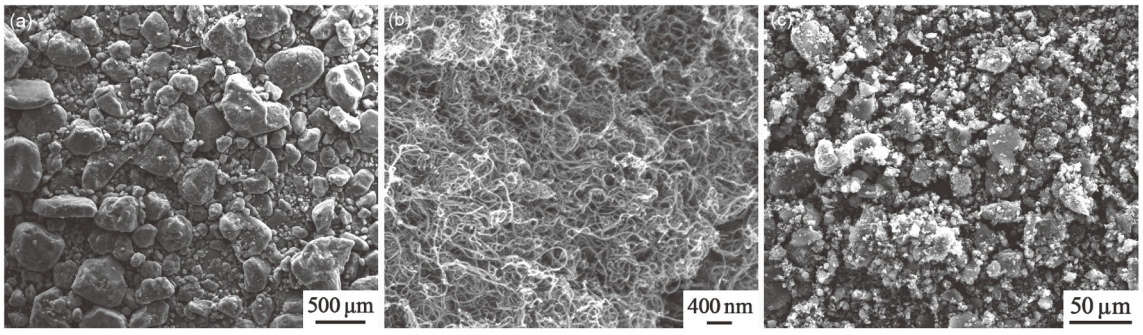

Figure 1 SEM images of the raw CNT ((a), (b)) and PS-CNT powders (c).

at 803 K for 2 h, quenched in water at room temperature and then artificial aging treated at 443 K for 6 h (T6 treatment). For comparison, 6061Al alloy was also fabricated and heat treated under the same hot densification and heat treatment processing.

2.2 Wear tests and characterization of the CNT/6061Al composites

The experimental approach of the wear testing is shown in Figure 3. The wear tests for CNT/6061Al were performed by a pin-on-disk type wear tester (MM-W1A vertical friction and wear testing machine) at room temperature. The wear samples of CNT/6061Al composites were sectioned along the hot extrusion direction and machined to cylindrical pins with a diameter of 4.7 mm and a height of 15 mm. Aluminum bronze annular disks with a hardness of 253 HV were used as a wear counterpart. The cylindrical pins and the counterpart surface were polished with 1000 mesh SiC paper and then degreased with acetone before testing. The tests were carried out under dry sliding condition at a constant sliding speed of 0.5 m s^{-1}. The maximum sliding distance was 600 m and applied loads ranging from 5 to 15 N. The wear rates of CNT/6061Al composites were determined from the following equation [26]:

$$K = \frac{\Delta m}{\rho \cdot L}, \tag{1}$$

where K (mm^{-3} m^{-1}) is the wear rate, Δm (g) is the mass loss of composite sample after the wear test, ρ (g cm^{-3}) is the density of composite, L (m) is the sliding distance. The weight of the specimens was measured before and after the wear tests using a digital balance with an accuracy of 0.001 mg.

Scanning electron microscopy (SEM, Quanta 450) with energy dispersive spectroscopy (EDS) was used to characterize the CNT distributions, wear surface, cross-section of wear samples, counterpart surface, and wear debris. The samples for observing CNT distributions were corroded by

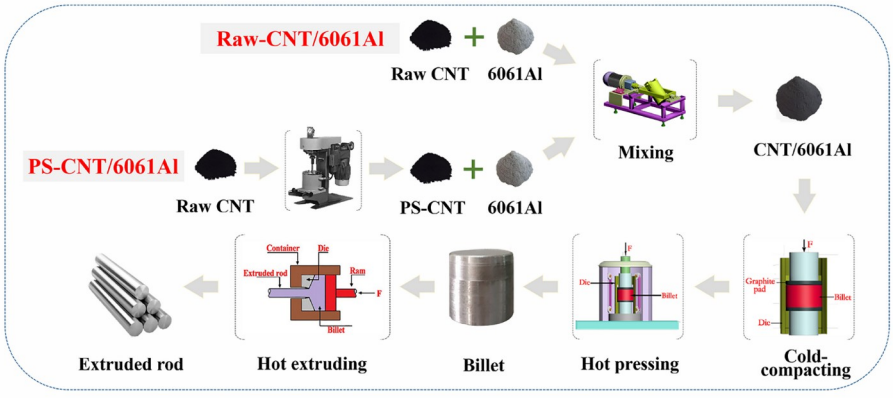

Figure 2 (Color online) Schematic illustration for the fabrication routes of the CNT/6061Al composites.

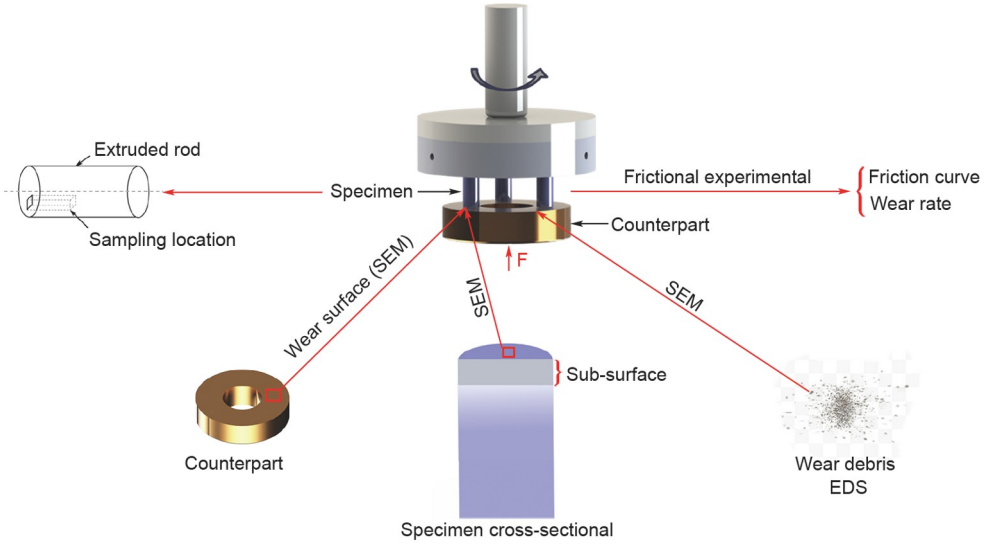

Figure 3 (Color online) Schematic of the experimental approach of wear test.

Keller reagent. The samples after wear were machined along the axial direction (Figure 3) and then inlaid with mounting material for observing the cross-section of the wear surfaces. The densities of the composite samples were measured by using the Archimedes principle, and the hardness was measured at eight points using a Vickers hardness tester (FM-700, a load of 200 g and a dwell time of 15 s) to obtain an average value.

3 Results and discussion

3.1 CNT distribution in composites

Figure 4 shows the distribution of CNT in CNT/6061Al composites with different CNT contents under different fabrication routes. For the raw-CNT/6061Al composites, the CNT clusters with strip shapes could be observed, and the CNT cluster strips were aligned along the extrusion direction. Further, the length and width of the CNT cluster strips increased with increasing the CNT content (Figure 4(b)–(d)). Compared with the raw-CNT/6061Al composites, the PS-CNT/6061Al composites had much smaller CNT clusters, as shown in Figure 4(e)–(g). The typical magnified images of CNT clusters in 1 wt.% raw-CNT/6061Al composite are shown in Figure 4(h) and (i). It is clear that no Al could be extruded into the large CNT clusters, and many micro-pores were observed in the CNT clusters. Obviously, too many of the large CNT clusters had a negative impact on the composites.

3.2 CNT/6061Al density and hardness

Figure 5 shows the density and Vicker's hardness of the CNT/6061Al composites with different CNT contents.

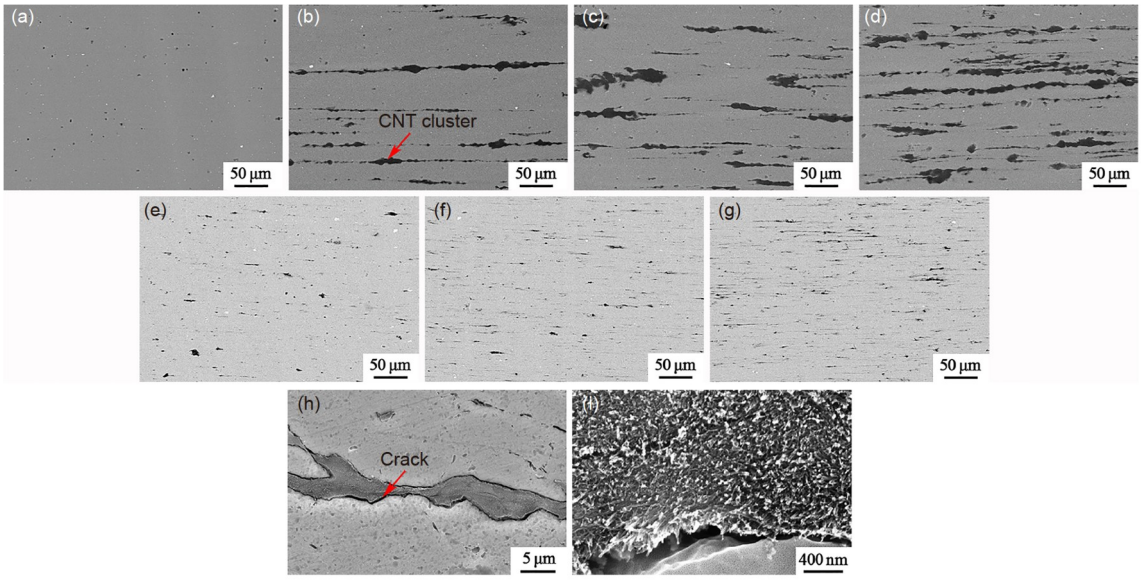

Figure 4 (Color online) Back scatter SEM images showing morphologies of the raw-CNT/6061Al composites with different CNT contents: (a) 0 wt.%; (b) 1 wt.%; (c) 2 wt.%; (d) 3 wt.%; the PS-CNT/6061Al composites with different CNT contents: (e) 1 wt.%; (f) 2 wt.%; (g) 3 wt.%; (h), (i) the magnified images of 1 wt.% raw-CNT/6061Al composite.

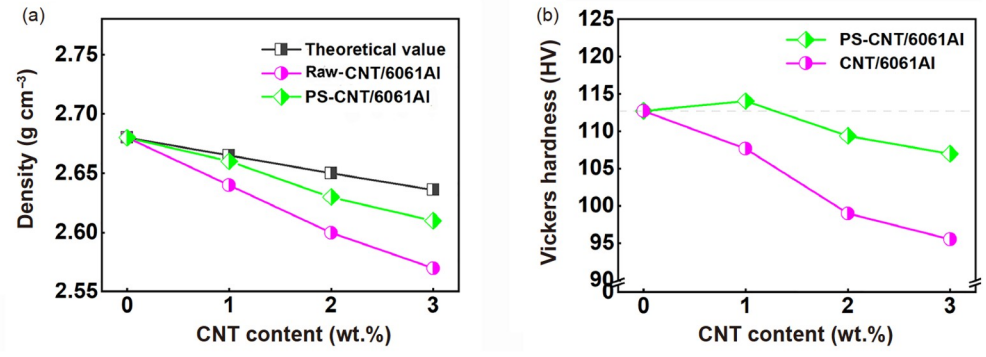

Figure 5 Density (a) and Vicker's hardness (b) of the raw-CNT/6061Al and PS-CNT/6061Al composites with different CNT contents.

Obviously, the composite density decreases with the increase of the CNT content, for either the raw-CNT/6061Al or the PS-CNT/6061Al. This could have resulted from two aspects. On one hand, CNT had a lower density than the 6061Al matrix, which could be reflected by the theoretical density change calculated by the rule of mixture. On the other hand, CNT clusters were rich of micro-pores, which could not be well filled with the 6061Al matrix. This is the reason why the experimental density was lower than the theoretical density. Compared with the raw CNT, the pre-smashed CNT significantly improved the density of CNT/6061Al composites (Figure 5(a)). This was mainly for the significant decrease of CNT cluster size, which effectively decreased the porosity of CNT/6061Al composites.

For the raw-CNT/6061Al composites, the Vicker's hardness decreased as the CNT content increasing. This was mainly due to the fact that there were too many micro-pores in the large CNT clusters, and the CNT could not play the role of load transferring. For the PS-CNT/6061Al composites, 1 wt.% CNT incorporation could slightly increase the Vicker's hardness, however, the Vicker's hardness began to decrease with further increasing the CNT content. Compared with the raw-CNT/6061Al, the hardness of the PS-CNT/6061Al composites was greatly improved.

It was believed that some of the finer CNT clusters with fewer pores could transfer load and induce strengthening. Further, the appropriate content of CNT with smaller entangled size played an important role in hardness strengthening because of the grain refining resulted from the CNT-induced recrystallization [31,33]. The smaller CNT cluster resulted in the increase of contact area between PS-CNT and 6061Al, which increased the ratio of recrystallization. However, excess PS-CNT would induce large numbers of clusters, and the porosity of PS-CNT/6061Al composites would also significantly increase [17,34–36]. The above results indicate that reducing the size of CNT clusters could significantly improve the density and hardness of CNT/6061Al composites.

3.3 CNT/6061Al wear behavior

Figures 6 and 7 show the friction coefficient of the CNT/6061Al composites with different CNT contents under an applied load of 15 N, at a sliding speed of 0.5 m s^{-1}. For the raw-CNT/6061Al composites (Figure 6), the friction coefficient showed considerable variation. As the wear test carried on till two-third of the test, the friction coefficient curves leaped and the friction coefficient increased dramatically. This indicates the transition of the wear mechanism, and it will be discussed in the following section. By contrast, the friction coefficient curves for the PS-CNT/6061Al composites (Figure 7) were relatively stable and there was no exceptional volatility.

Wear rates for the raw-CNT/6061Al and PS-CNT/6061Al composites as a function of CNT content under different applied loads are shown in Figure 8(a) and (b). On the whole, the wear rate of CNT/6061Al composites increased as the applied load was increased from 5 to 15 N. For the raw-CNT/6061Al composites, the wear rate increased approximately linear trend as the CNT content was over 1 wt.%, and the wear rate increased dramatically with the increase of applied load. This was in accordance with the results reported by Yildirim et al. [27]. This is mainly attributed to the presence of pores as well as the large CNT clusters in the composites. The pores and CNT clusters served as a source of crack nucleation, which resulted in poor wear resistance of the composites. Moreover, weaker bonding between CNT clusters and 6061Al could be another reason for its excessive subsurface fracturing at higher loads [37].

For the PS-CNT/6061Al composites, the wear rate decreased gradually as the CNT content was lower than 2 wt.%. These results showed that pre-smashing processing significantly improved the wear resistance of CNT/6061Al composites compared with those of the raw-CNT/6061Al composites. But the wear rate increased significantly when the CNT content was 3 wt.%, especially under a higher applied load of 15 N.

Figure 8(c) shows the friction coefficient curves of PS-CNT/6061Al composites under different applied loads. The friction coefficient changing curves showed a similar tendency to the wear rate change curves with the change of CNT content. The friction coefficient increased first and then decreased with the increase of applied load.

Figure 9 shows the wear surface of the raw-CNT/6061Al composites with different CNT contents under 15 N. It revealed that many grooves formed on the wear surface of the 6061Al sample, and many counterpart materials were found to adhere to the wear surfaces of the 6061Al samples (Figure 9(a) and (e)). This indicated that abrasive wear and adhesive wear were the dominated wear mechanism for the matrix alloy under an applied load of 15 N. For the 1 wt.% of raw-CNT/6061Al composite, deeper and wider grooves without adhesive counterpart materials could be clearly seen on the wear surface, which indicates that the wear mechanism was dominated by abrasive wear. It was believed that the addition of CNTs inhibited the direct contact between the sample and counterpart material, which weakened the adhesion-binding energy between aluminum and copper (455×10^{-3} J m^{-2}) [36,38–43]. This could also be proved by the existence of the entangled CNT particles on the wear surface (Figure 9(f)).

But for the raw-CNT/6061Al composites with 2 wt.% and 3 wt.% CNTs, the severe plastic deformation, deeper grooves, and serious delamination could be observed on the wear surface. This could attribute to the increased number of larger CNT clusters rich in micro-pores. Moreover, the weak interfacial bonding between CNT clusters and 6061Al

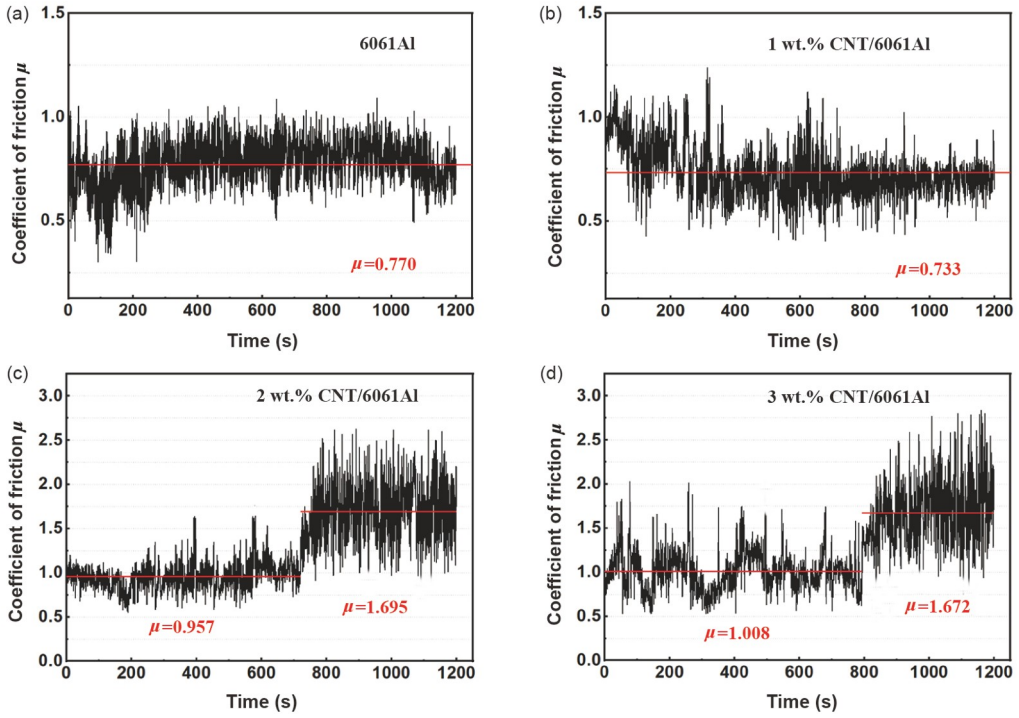

Figure 6 The friction coefficients versus the sliding time for the raw-CNT/6061Al composites with different CNT contents under 15 N.

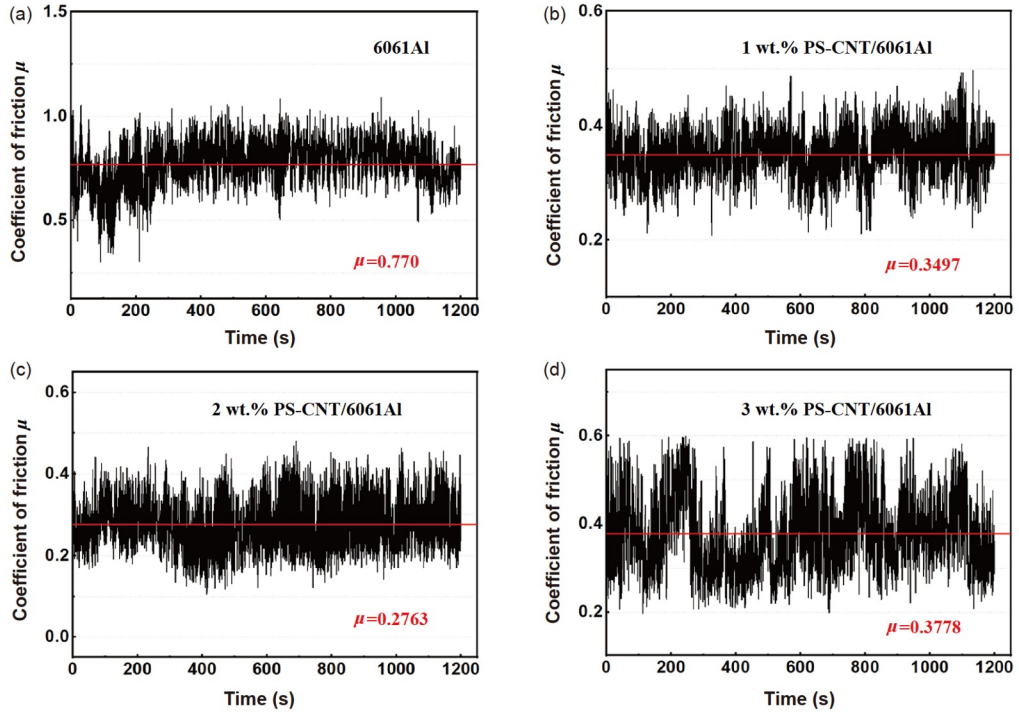

Figure 7 (Color online) The friction coefficients versus the sliding time for the PS-CNT/6061Al composites with different CNT contents under 15 N.

resulted in much lower hardness and weaker anti-shearing plastic deformation ability of composites, which prompted crack initiation and propagation at higher load [15,17,18,36].

Figure 10 shows the SEM images of wear surfaces of the PS-CNT/6061Al composites with different CNT contents under 15 N. It can be seen that the adhesive counterpart

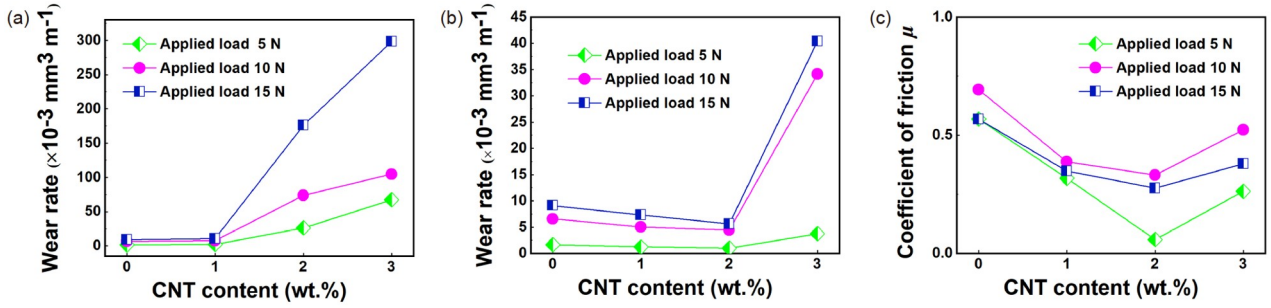

Figure 8 (Color online) Wear rate changing curves of the raw-CNT/6061Al composites (a), the PS-CNT/6061Al composites (b), and the friction coefficient curves of PS-CNT/6061Al composites (c) under different applied loads.

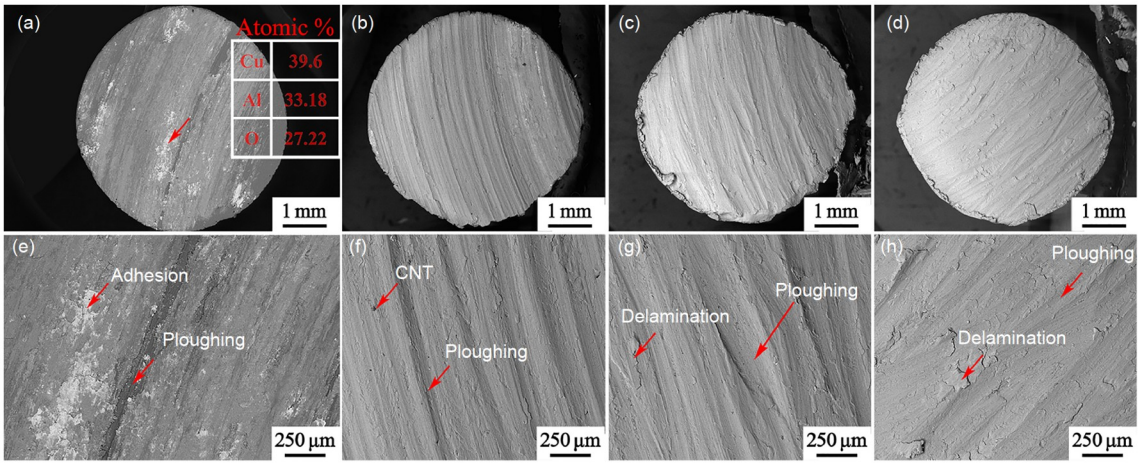

Figure 9 (Color online) Back scatter SEM images of wear surfaces of the raw-CNT/6061Al composites with different CNT contents under 15 N. (a), (e) Matrix alloy; (b), (f) 1 wt.%; (c), (g) 2 wt.%; (d), (h) 3 wt.%. White phase was counterpart material.

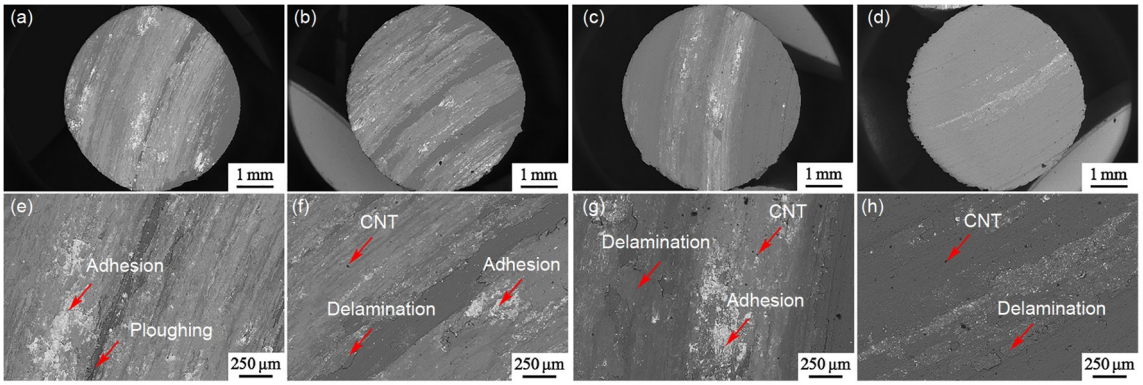

Figure 10 (Color online) Back scatter SEM images of wear surfaces of PS-CNT/6061Al composites with different CNT contents under 15 N. (a), (e) Matrix alloy; (b), (f) 1 wt.%; (c), (g) 2 wt.%; (d), (h) 3 wt.%. White phases were the counterpart materials adhered on the wear surfaces.

materials on the wear surface decreased gradually with the increase of CNT content. Compared with the raw-CNT/6061Al, the grooves on the wear surfaces of the PS-CNT/6061Al caused by plowing were much shallower, and no significantly plastic deformation could be observed. In particular, for the 3 wt.% PS-CNT/6061Al composite, the CNT exposed on the wear surface was relatively fewer and there was mild plastic deformation, which could result from the excessive delamination wear. Overall, pre-smashing processing significantly improved the wear resistance of CNT/6061Al composites during the wear process. Appropriate PS-CNT content prevented the direct contact between sample and counterpart material, which effectively inhibited the adhesive wear [36,44]. But excess PS-CNT would still induce a large number of the porosity in the PS-CNT/6061Al composites, which resulted in the reduction of the strength of

the PS-CNT/6061Al, thereby leading to the poor wear resistance.

The wear surfaces of counterparts are shown in Figure 11. For the raw-CNT/6061Al composites, the composites (the dark color) adhered to the counterpart increased gradually with the increase of CNT content. Especially, for the 2 wt.% and 3 wt.% CNT/6061Al composites, the wear surfaces of the counterparts were almost fully covered by the composite materials. It means that the wear process was gradually transformed from Al-copper base counterpart wear into Al-Al wear during the wear test. This was also in accordance with the fact that the friction coefficient leaped significantly at the two-third of the wear process, as shown in Figure 6(c) and (d). The high adhesion-binding energy between aluminum and aluminum (525×10^{-3} J m^{-2}) was the main reason for the leap phenomenon of the friction coefficient curves.

For the PS-CNT/6061Al composites, the composite adhered on the wear surfaces of the counterpart decreased gradually with the increase of CNT content from 0 to 2 wt.%. But for the 3 wt.% PS-CNT/6061Al composites, the adhesion of composite increased dramatically, which was in accordance with the changing curve of wear rate (Figure 8(b)).

Figure 12 shows the SEM images of wear debris of the raw-CNT/6061Al and PS-CNT/6061Al composites with different CNT contents under 15 N. For either the raw-CNT/6061 Al or PS-CNT/6061Al, the counterpart material (brighter color) in the wear debris decreased gradually with the increase of CNT contents, which could be reflected by the change of Cu element based on the EDX results of the wear debris showing in Figure 13. For the raw-CNT/6061Al composites, the wear debris size increased with the increase of CNT contents, which mainly attributed to the reduction of anti-shearing plastic deformation ability. The O element content decreased gradually with the increase of CNT content. In general, the oxide layer was reported due to frequent fracturing and delamination of material from the sample surface [16,19]. This indicates that the oxidation wear was significantly inhibited.

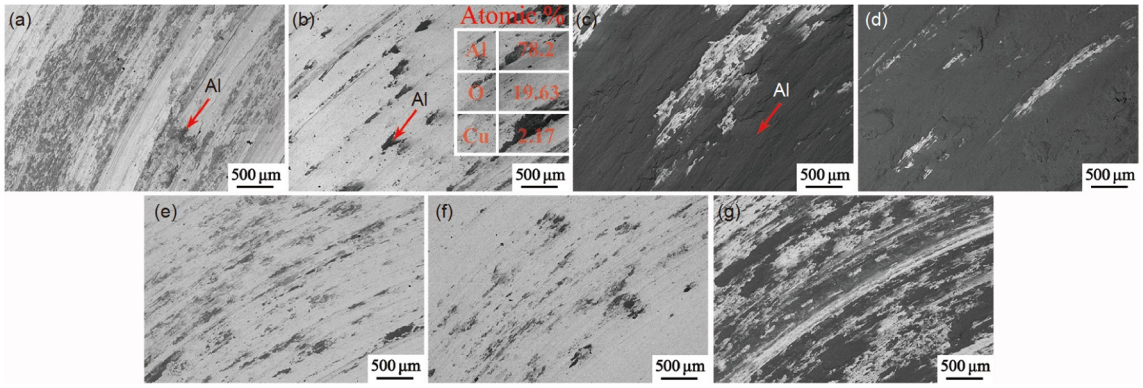

Figure 11 (Color online) Back scatter SEM images of wear surface of the raw-CNT/6061Al composite counterparts: (a) matrix alloy; (b) 1 wt.%; (c) 2 wt.%; (d) 3 wt.%; PS-CNT/6061Al composite counterparts: (e) 1 wt.%; (f) 2 wt.%; (g) 3 wt.%.

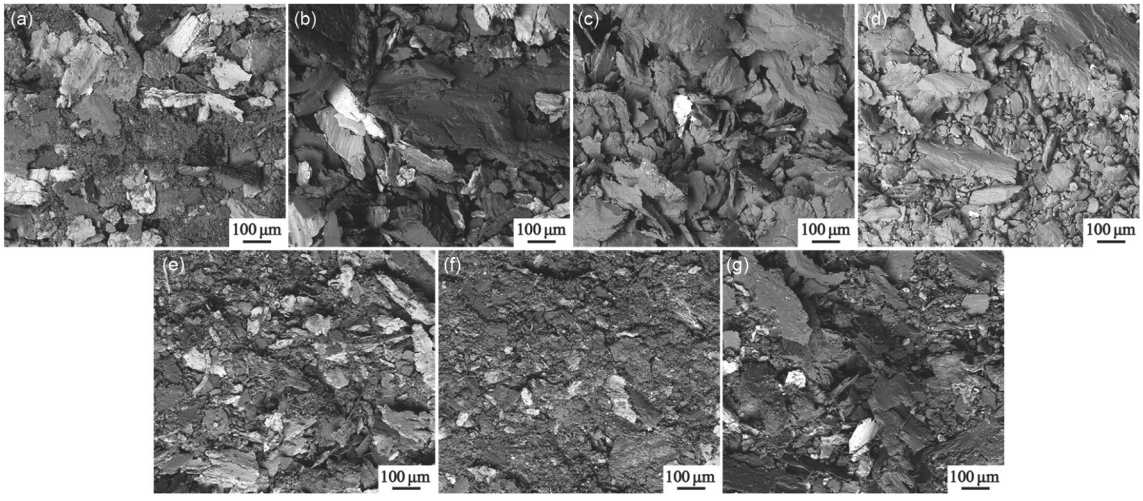

Figure 12 Back scatter SEM images of the wear debris morphologies of the raw-CNT/6061Al composites for (a) 0 wt.%; (b) 1 wt.%; (c) 2 wt.%; (d) 3 wt.%; and the PS-CNT/6061Al composites for (e) 1 wt.%; (f) 2 wt.%; (g) 3 wt.%.

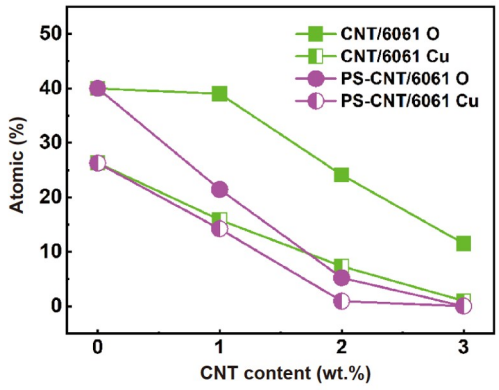

Figure 13 (Color online) Cu and O element contents in the wear debris of the raw-CNT/6061Al and PS-CNT/6061Al composites with different CNT contents under 15 N.

But for the PS-CNT/6061Al composites, the wear debris size decreased first and then increased significantly (3 wt.%) with the increase of CNT content (Figure 12(e)–(g)). And the O element content decreased with increasing the CNT content, indicating that adding CNT inhibited the oxidation wear significantly (Figure 13).

Figure 14 shows the wear subsurface cross-sections of CNT/6061Al composites. The mechanically mixed layer (MML) generated for the matrix alloy, 1 wt.% and 2 wt.% PS-CNT/6061Al composites, which had excellent friction reducing and wear resistant effects [45–47]. For the matrix alloy, MML composed of debris (Figure 14(a) and (h)), which fractured and comminuted continually from both sides of the contact surfaces. The alternate stacking of composites and counterpart materials was the chief reason for the generation of the MML [48,49].

The area and thickness of the MML (Figure 14(h)) for the matrix alloy were larger compared with those of the 1 wt.% PS-CNT/6061Al composites, which resulted in the crack initiation and lower adhesive strength of the MML. Instead, the few stacked layers with fine debris (Figure 14(i)) provided larger adhesive strength. Adding 2 wt.% PS-CNT reduced the thickness of the MML and the wear rate of the corresponding composite dramatically decreased, which generated finer debris as illustrated in Figure 12(e) and (f).

4 Conclusions

Reducing the CNT cluster size by pre-smashing processing could effectively improve the density, hardness, and wear resistance of the PS-CNT/6061Al composites. For either the raw-CNT/6061Al or the PS-CNT/6061Al, the wear rate increased as the applied load was increased from 5 to 15 N.

For the raw-CNT/6061Al composites, the wear rate increased approximately linear trend when the CNT content was over 1 wt.%. Abrasive wear and adhesive wear were the dominant wear mechanisms for the matrix alloy, while the

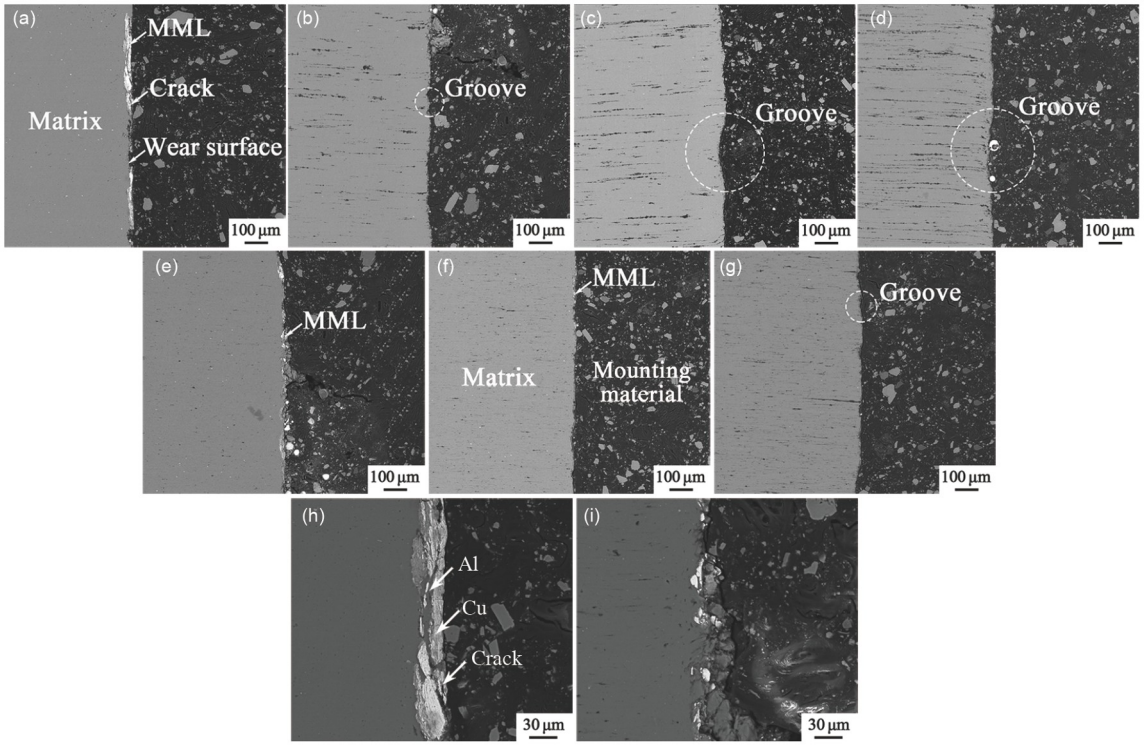

Figure 14 The wear subsurface cross-sections of the raw-CNT/6061Al composites for (a) 0 wt.%, (b) 1 wt.%, (c) 2 wt.%, (d) 3 wt.%, and PS-CNT/6061Al composites for (e) 1 wt.%, (f) 2 wt.%, (g) 3 wt.% under 15 N; the magnified images of (h) 0 wt.% and (i) 1 wt.% PS-CNT/6061Al composites.

abrasive wear was the dominant wear mechanism for the 1 wt.% raw-CNT/6061Al composites. But for the 2 wt.% and 3 wt.% raw-CNT/6061Al composites, the plastic deformation, deep grooves, and serious delamination were presented on the wear surfaces.

For the PS-CNT/6061Al composites, the wear rate decreased gradually as the CNT content was lower than 2 wt.%, and increased dramatically as the CNT content was 3 wt.%. The abrasive wear and adhesive wear were the dominant wear mechanisms, and the adhesive counterpart materials on the wear surface decreased gradually with the increase of CNT content. Appropriate PS-CNT content prevented the direct contact between the composite sample and counterpart material, which effectively inhibited the adhesive wear. But excess PS-CNT content would induce a large number of porosity and CNT clusters, and thus the composites' wear resistance decreased dramatically.

This work was supported by the National Key R&D Program of China (Grant No. 2017YFB0703104), the Key Research Program of Frontier Sciences, CAS (Grant No. QYZDJ-SSW-JSC015), the National Natural Science Foundation of China (Grant Nos. 51931009, 51871214, 51871215), and the Youth Innovation Promotion Association CAS (Grant No. 2020197).

1 Xiao B L, Huang Z Y, Ma K, et al. Research on hot deformation behaviors of discontinuously reinforced aluminum composites. Acta Metall Sin, 2019, 55: 59–72
2 Zan Y N, Zhou Y T, Liu Z Y, et al. Enhancing strength and ductility synergy through heterogeneous structure design in nanoscale Al_2O_3 particulate reinforced Al composites. Mater Des, 2019, 166: 107629
3 Zan Y N, Zhou Y T, Li X N, et al. Enhancing high-temperature strength and thermal stability of Al_2O_3/Al composites by high-temperature pre-treatment of ultrafine Al powders. Acta Metall Sin (Engl Lett), 2020, 33: 913–921
4 Miyajima T, Iwai Y. Effects of reinforcements on sliding wear behavior of aluminum matrix composites. Wear, 2003, 255: 606–616
5 Zhou L, Cui C, Wang Q Z, et al. Constitutive equation and model validation for a 31 vol.% B_4Cp/6061Al composite during hot compression. J Mater Sci Tech, 2018, 34: 1730
6 Bakshi S R, Lahiri D, Agarwal A. Carbon nanotube reinforced metal matrix composites—A review. Int Mater Rev, 2013, 55: 41–64
7 Singla D, Amulya K, Murtaza Q. CNT reinforced aluminium matrix composite—A review. Mater Today-Proc, 2015, 2: 2886–2895
8 Tjong S C. Recent progress in the development and properties of novel metal matrix nanocomposites reinforced with carbon nanotubes and graphene nanosheets. Mater Sci Eng-R-Rep, 2013, 74: 281–350
9 Choi H, Kwon G, Lee G, et al. Reinforcement with carbon nanotubes in aluminum matrix composites. Scripta Mater, 2008, 59: 360–363
10 Akhlaghi F, Zare-Bidaki A. Influence of graphite content on the dry sliding and oil impregnated sliding wear behavior of Al 2024-graphite composites produced by *in situ* powder metallurgy method. Wear, 2009, 266: 37–45
11 Zhao K, Liu Z Y, Xiao B L, et al. Origin of insignificant strengthening effect of CNTs in T6-treated CNT/6061Al composites. Acta Metall Sin (Engl Lett), 2017, 31: 134–142
12 Zhang X X, Zhang J F, Liu Z Y, et al. Microscopic stresses in carbon nanotube reinforced aluminum matrix composites determined by *in-situ* neutron diffraction. J Mater Sci Tech, 2020, 54: 58–68
13 Nam D H, Kim J H, Cha S I, et al. Hardness and wear resistance of carbon nanotube reinforced aluminum-copper matrix composites. J Nanosci Nanotechnol, 2014, 14: 9134–9138
14 Bakshi S R, Agarwal A. An analysis of the factors affecting strengthening in carbon nanotube reinforced aluminum composites. Carbon, 2011, 49: 533–544
15 Zhou S, Zhang X, Ding Z, et al. Fabrication and tribological properties of carbon nanotubes reinforced Al composites prepared by pressureless infiltration technique. Compos Part A-Appl Sci Manuf, 2007, 38: 301–306
16 Bastwros M M H, Esawi A M K, Wifi A. Friction and wear behavior of Al-CNT composites. Wear, 2013, 307: 164–173
17 Kim I Y, Lee J H, Lee G S, et al. Friction and wear characteristics of the carbon nanotube-aluminum composites with different manufacturing conditions. Wear, 2009, 267: 593–598
18 Chen W X, Tu J P, Wang L Y, et al. Tribological application of carbon nanotubes in a metal-based composite coating and composites. Carbon, 2003, 41: 215–222
19 Al-Qutub A M, Khalil A, Saheb N, et al. Wear and friction behavior of Al6061 alloy reinforced with carbon nanotubes. Wear, 2013, 297: 752–761
20 Pérez-Bustamante R, Bueno-Escobedo J L, Jiménez-Lobato J, et al. Wear behavior in Al2024-CNTs composites synthesized by mechanical alloying. Wear, 2012, 292-293: 169–175
21 Choi H J, Lee S M, Bae D H. Wear characteristic of aluminum-based composites containing multi-walled carbon nanotubes. Wear, 2010, 270: 12–18
22 Suzuki T, Kato M, Saito H, et al. Effect of carbon nanotube (CNT) size on wear properties of Cu-based CNT composite electrodes in electrical discharge machining. JMMP, 2011, 5: 348–359
23 Sundaram R, Yamada T, Hata K, et al. Electrical performance of lightweight CNT-Cu composite wires impacted by surface and internal Cu spatial distribution. Sci Rep, 2017, 7: 9267
24 Liu Z Y, Ma K, Fan G H, et al. Enhancement of the strength-ductility relationship for carbon nanotube/Al-Cu-Mg nanocomposites by material parameter optimisation. Carbon, 2020, 157: 602–613
25 Liu Z Y, Zhao K, Xiao B L, et al. Fabrication of CNT/Al composites with low damage to CNTs by a novel solution-assisted wet mixing combined with powder metallurgy processing. Mater Des, 2016, 97: 424–430
26 Jiang J L, Wang H Z, Yang H, et al. Fabrication and wear behavior of CNT/Al composites. Trans Nonferr Metals Soc China, 2007, 17: 113–116
27 Yildirim M, Özyürek D, Gürü M. Investigation of microstructure and wear behaviors of al matrix composites reinforced by carbon nanotube. Fullerenes Nanotubes Carbon Nanostruct, 2016, 24: 467–473
28 Idusuyi N, Olayinka J I. Dry sliding wear characteristics of aluminium metal matrix composites: A brief overview. J Mater Res Tech, 2019, 8: 3338–3346
29 Morsi K, Esawi A. Effect of mechanical alloying time and carbon nanotube (CNT) content on the evolution of aluminum (Al)-CNT composite powders. J Mater Sci, 2007, 42: 4954–4959
30 Liu Z Y, Xu S J, Xiao B L, et al. Effect of ball-milling time on mechanical properties of carbon nanotubes reinforced aluminum matrix composites. Compos Part A-Appl Sci Manuf, 2012, 43: 2161–2168
31 Liu Z Y, Xiao B L, Wang W G, et al. Analysis of carbon nanotube shortening and composite strengthening in carbon nanotube/aluminum composites fabricated by multi-pass friction stir processing. Carbon, 2014, 69: 264–274
32 Liu Z Y, Xiao B L, Wang W G, et al. Tensile strength and electrical conductivity of carbon nanotube reinforced aluminum matrix composites fabricated by powder metallurgy combined with friction stir processing. J Mater Sci Tech, 2014, 30: 649–655
33 Ramesh C S, Keshavamurthy R, Koppad P G, et al. Role of particle stimulated nucleation in recrystallization of hot extruded Al 6061/SiCp composites. Trans Nonferrous Met Soc China, 2013, 23: 53–58
34 Wang L Y, Tu J P, Chen W X, et al. Friction and wear behavior of electroless Ni-based CNT composite coatings. Wear, 2003, 254: 1289–1293

35 Liu Y B, Lim S C, Ray S, et al. Friction and wear of aluminium-graphite composites: The smearing process of graphite during sliding. Wear, 1992, 159: 201–205
36 Vijh A K. The influence of metal-metal bond energies on the adhesion, hardness, friction and wear of metals. J Mater Sci, 1975, 10: 998–1004
37 He H, Hahn S H, Yu J, et al. Friction-induced subsurface densification of glass at contact stress far below indentation damage threshold. Acta Mater, 2020, 189: 166–173
38 Pashley M D, Pethica J B, Tabor D. Adhesion and micromechanical properties of metal surfaces. Wear, 1984, 100: 7–31
39 Derjaguin B V, Smilga V P. Electronic theory of adhesion. J Appl Phys, 1967, 38: 4609–4616
40 Kayaba T, Kato K. Wear of Materials. New York: ASME, 1979. 45
41 Rigney D A, Chen L H, Naylor M G S, et al. Wear processes in sliding systems. Wear, 1984, 100: 195–219
42 Chen L H, Rigney D A. Transfer during unlubricated sliding wear of selected metal systems. Wear, 1985, 105: 47–61
43 Tabor D. Surface forces and surface interactions. J Colloid Interface Sci, 1977, 58: 2–13
44 Pei Y T, Galvan D, De Hosson J T M. Nanostructure and properties of TiC/a-C:H composite coatings. Acta Mater, 2005, 53: 4505–4521
45 Venkataraman B, Sundararajan G. Correlation between the characteristics of the mechanically mixed layer and wear behaviour of aluminium, Al-7075 alloy and Al-MMCs. Wear, 2000, 245: 22–38
46 Lee T, Lee J, Lee D, et al. Effects of particle size and surface modification of SiC on the wear behavior of high volume fraction Al/SiCp composites. J Alloys Compd, 2020, 831: 154647
47 Hassan A M, Mayyas A T, Alrashdan A, et al. Wear behavior of Al-Cu and Al-Cu/SiC components produced by powder metallurgy. J Mater Sci, 2008, 43: 5368–5375
48 Zhang J, Alpas A T. Transition between mild and severe wear in aluminium alloys. Acta Mater, 1997, 45: 513–528
49 Yin C, Liang Y, Liang Y, et al. Formation of a self-lubricating layer by oxidation and solid-state amorphization of nano-lamellar microstructures during dry sliding wear tests. Acta Mater, 2019, 166: 208–220